Chapter 2
Application of High Performance Computing to Rapid Assessment of Tunnel Vulnerability to Explosive Blast and Mitigation Strategies

L. Glascoe and T. Antoun

Abstract To credibly assess tunnel vulnerabilities to explosives and the mitigation of these vulnerabilities, one must consider the energetic source of the shock, the geophysical response of the surrounding soil or rock under strong dynamic loading, and the structural and material response of the tunnel to the explosion. Tools used for such assessments often require significant computational resources and expert analyses. This chapter provides a concise overview of some recent high fidelity multiphysics approaches to modeling tunnel structures and the need for careful experimental validation of these models. Presented also is an example of how the building of reduced order models from these higher fidelity capabilities can help to quickly estimate the effects of explosions within carefully defined tunnel scenarios.

2.1 Introduction

High performance computational multiphysics analysis tools, e.g., the ALE3D, GEODYN, LDEC, DYNA3D, and CTH codes (Nichols and The ALE3D team 2009; Lomov et al. 2005; Lin 2005; McGlaun et al. 1990; Morris and Johnson 2009), are useful for describing and predicting the response of geology and structures to shock loads, and, if properly validated and caveated, can be used for vulnerability assessments and corrective measures to reduce overall risk (e.g., Noble et al. 2008; Glascoe et al. 2009, 2011; McMichael et al. 2009). To credibly assess tunnel vulnerability and mitigation, one must consider the energetic source of the shock, the physics of geologic response to strong dynamic loads, and, ultimately, the physics of structural and material response and failure resulting from dynamic shock loading events.

L. Glascoe, Ph.D., P.E. (✉) • T. Antoun
Lawrence Livermore National Laboratory, Box 808, L-126 7000
East Avenue, Livermore, CA 94550, USA
e-mail: Glascoe1@llnl.gov; Antoun1@llnl.gov

A. Shukla et al. (eds.), *Blast Mitigation: Experimental and Numerical Studies*,
DOI 10.1007/978-1-4614-7267-4_2, © Springer Science+Business Media New York 2014

As these tools require significant computational resources, timely assessment involving a large range of threats and threat locations is difficult. Further, high fidelity tools are typically deterministic in nature and, therefore, must assume a specified set of material properties for the structure itself. Consequently, there is a need for (1) careful experimental validation of relevant phenomena used in the high fidelity models, and (2) reduced order capabilities that can rapidly evaluate effects associated with various threat sizes, threat locations, and system states while quickly highlighting uncertainties associated with structural and system response. This chapter presents an overview of high fidelity multiphysics modeling for tunnel structures and the need for careful experimental validation, as well as the building of reduced order models (ROMs) from these higher fidelity capabilities to quickly estimate the effects of explosions within a contiguous system of confined spaces such as tunnels.

2.2 Multiphysics Models and High Performance Computing

Most civil structures, and, in particular, tunnels are not designed to withstand the intense dynamic loads produced by an explosive detonation in the vicinity of the structure. These impulsive loads are significantly different in magnitude and duration from those expected under service conditions, and consequently they induce deformation modes and damage mechanisms not normally experienced by the structure. Conventional engineering mechanics and structural analysis techniques are not adequate for assessing tunnel vulnerability under these severe loading conditions. Novel methods that can account for the prevalent dynamic loading phenomena and their nonlinear interactions are required to assess tunnel vulnerability.

Scenarios of interest are initiated by an explosive detonation either inside or outside the structure but usually in close proximity. This is followed by the propagation of a blast wave in the case of an internal detonation, or a ground shock in the case where the explosive charge is placed outside the structure. The energy coupling associated with the interaction of those waves with the tunnel can cause damage to various elements of the structure, sometimes leading to catastrophic collapse. Assessing tunnel vulnerability therefore requires the ability to analyze the explosive detonation, the propagation of the stress waves, and the response of the tunnel. In short, one must be able to solve a multiphysics problem involving several nonlinear, interacting phenomena. Multiphysics hydrocodes are ideally suited for addressing this class of problems, and the remainder of this section is dedicated to the description of the modeling approach and the challenges associated with the various phases of the analysis.

2.2.1 Modeling the Energetic Material Source

Capturing the response of energetic materials in simulations of tunnel vulnerability is essential to ensure accurate representation of the time-dependent release of chemical energy, the ensuing blast effects, and the eventual coupling of the released

energy into the structure. A wide array of explosives with widely varying energy densities and thermodynamic properties are usually considered in these simulations, ranging from military explosives and ANFO (ammonium nitrate–fuel oil), to improvised and homemade explosives.

For events triggered by explosives, the most important aspects of the behavior of the explosive are the energy release characteristics of the explosive and the pressure–volume response of the detonation product. For ideal explosives, these can be adequately described with a phenomenological equation of state calibrated using empirical data. The equation of state (EOS) most often used for this purpose is the Jones-Wilkins-Lee (JWL) EOS (Lee et al. 1968). The JWL EOS is an empirical pressure–volume equation that describes the adiabatic expansion of the detonation products. This equation contains several fitting parameters that are calibrated using experimental data. Due to its relative simplicity, and also because it has been demonstrated to accurately represent the behavior of many explosives, the JWL EOS is widely available in practically all the hydrodynamic and structural dynamics codes used in simulations involving explosive detonations. Standardized procedures have also been developed to determine the JWL EOS parameters using Chapman–Jouguet state parameters and data from cylinder expansion tests (Lawrence Livermore National 2012).

JWL is an appropriate EOS for ideal explosives, i.e., explosives with a relatively high reaction rate, and once calibrated, this EOS can be used to describe detonation phenomena under a wide range of conditions and for practically all explosive configurations of interest in tunnel vulnerability assessments. However, the behavior of nonideal, i.e., relatively slower reacting, explosives is typically more complicated than that of an ideal explosive, with the response often varying with the size and geometric configuration of the explosive charge. Characterizing the behavior of nonideal explosives therefore requires the use of more complex models and more sophisticated testing procedures (e.g., Fig. 2.1), with the data used to improve the model and the model used to better characterize the response of the explosive during detonation.

Most improvised and homemade explosives are nonideal and some of their response features during and after detonation cannot be adequately represented using the JWL EOS formulation. For those types of explosives where kinetic and other nonideal effects are important, more sophisticated models like the JWL++ (Souers et al. 2000), which accounts for time dependent reaction in prompt detonations, or the ignition and growth model (Lee and Tarver 1980), which accounts for heterogeneous mesoscopic mechanisms (friction, pore collapse, strain localization, etc.) using a phenomenological continuum approach, can be used for more accurate representation in hydrodynamic simulations. Advanced computer codes have also been developed to calculate the properties and thermodynamic state in nonideal heterogeneous energetic mixtures. CHEETAH (Fried 1995) and its predecessor TIGER (Cowperthwaite and Zwisler 1974) are two codes that fall into this category, with CHEETAH being the current industry standard. CHEETAH is a thermochemical code which uses physical and chemical properties to predict the performance of ideal and nonideal high explosives and explosive formulations. It employs Chapman–Jouguet detonation theory and performs molecular calculations to determine bulk explosive properties like pressure and detonation velocity. The output from CHEETAH can be used to characterize explosive EOS properties in hydrodynamic calculations.

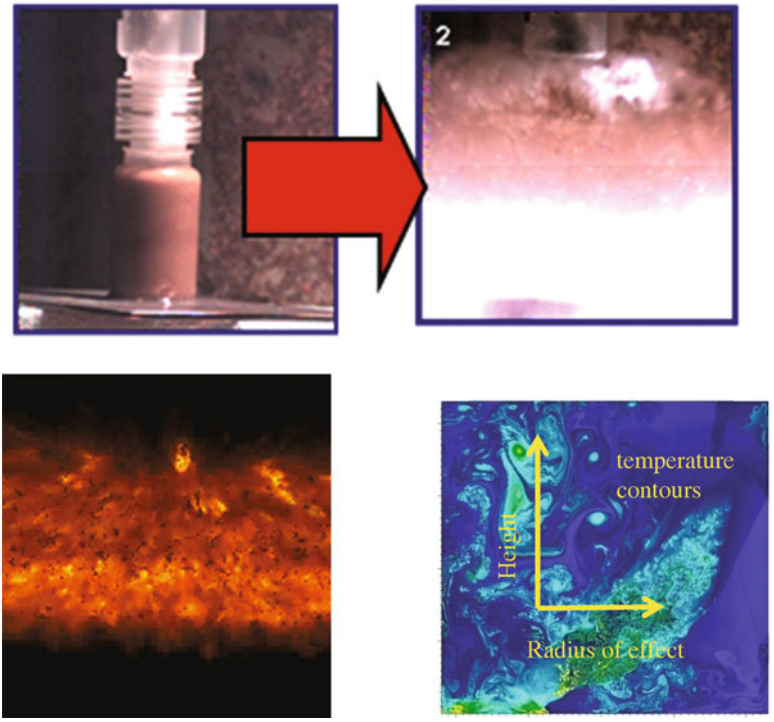


Fig. 2.1 Experimental (*top and lower left*) and numerical characterization (*lower right*) of nonideal explosives

Circumstances arise where the response of the explosive is highly nonideal, the reaction rates are variable and dependent on geometry and thermochemical state, and the EOS evolves with the rapidly changing local conditions. Under these circumstances, the thermochemical and hydrodynamic behaviors are fully coupled, and the notion of an EOS must be replaced with an approach that allows accurate representation of the coupled chemical and physical processes. Dynamic coupling of a thermochemical code like CHEETAH and a hydrodynamic code like ALE3D enables this important capability and allows accurate representation of the complex, interacting physical and chemical processes associated with the explosive detonation.

2.2.2 Modeling Geologic Materials

Earthen materials, including rock, sand and soils are the geologic settings in which tunnels are constructed. For this reason, the ability to accurately simulate the propagation of stress waves in geologic media, and the interaction of those waves with buried structures is of significant importance in assessing tunnel vulnerability and associated mitigation strategies. This requires the use of constitutive and failure

models that capture the behavior of geologic materials under dynamic loading conditions. Continuum mechanics based constitutive models are currently the only practical models for use in large scale (field scale) simulations of the dynamic response of geologic materials (e.g., Rubin et al. 2000). These models rely on fitting parameters to phenomenologically describe the dependence of processes like yielding, bulking, damage and porous compaction on the deformation history and the rate of load application.

The material response in these models is generally correlated to laboratory measured properties like density, elastic sound speed, stress–strain data under a range of loading conditions, and measurements of the strength and failure envelopes. Models calibrated in this manner can be shown to reproduce the behavior of the geologic medium under dynamic loading conditions, as shown in Fig. 2.2. The figure compares simulated and measured particle velocity and displacement histories at two different ranges away from an underground nuclear explosion in granite (Antoun et al. 1999, 2001). The data shown in the figure is from the PILE DRIVER underground nuclear test (Perret 1968), a 61 kt nuclear explosion detonated at a depth of 462.8 m in the Climax Stock granitic outcrop of Area 15 at the Nevada National Security Site (NNSS), formerly known as the Nevada Test Site (NTS). The data in Fig. 2.2a correspond to ground motion 204 m away from the center of detonation (ground zero) along the shot horizon. The data in Fig. 2.2b was collected along the same radial, at a distance of 470 m away from ground zero. The material behavior at both these ranges is inelastic, and as shown the model closely reproduces the response of the medium at the locations of these measurements. Once calibrated, the model can be used to represent the geologic medium in large scale simulations aimed at assessing the dynamic response of buried structures.

Geologic materials are highly heterogeneous, and when those heterogeneities are not properly represented in the small laboratory samples used to extract material property data for model calibration, the resulting constitutive model will not adequately represent field scale behavior where such heterogeneities may influence, and even dominate, the dynamic response. A common manifestation of this effect is that models developed using laboratory data have been shown to overpredict the free field environment in large scale field experiments in fractured granite. This is largely due to the effects of joints and other heterogeneities that are present at the field scale, but not in pristine laboratory samples. Indeed, the good agreement between the simulated and measured motions shown in Fig. 2.2 required modifications to the model parameters originally calibrated using the static laboratory data. Specifically, a scaling law was introduced to degrade the yield and strength surfaces as shown in Fig. 2.3.

Phenomenologically, this is in line with experimental data that show the strength of granite and other geologic materials to be size-dependent, decreasing with increasing specimen dimensions (e.g., Hoek 1994; Hoek and Brown 1980). However, the manner in which this size scaling was introduced into the model was empirical. A function was added to the model to represent this effect, and its parameters were calibrated to achieve good agreement with the free field wave propagation data.

This modeling approach, whereby mechanistic data are used to calibrate the model, and the calibrated model is used to shed insight into the behavior of the

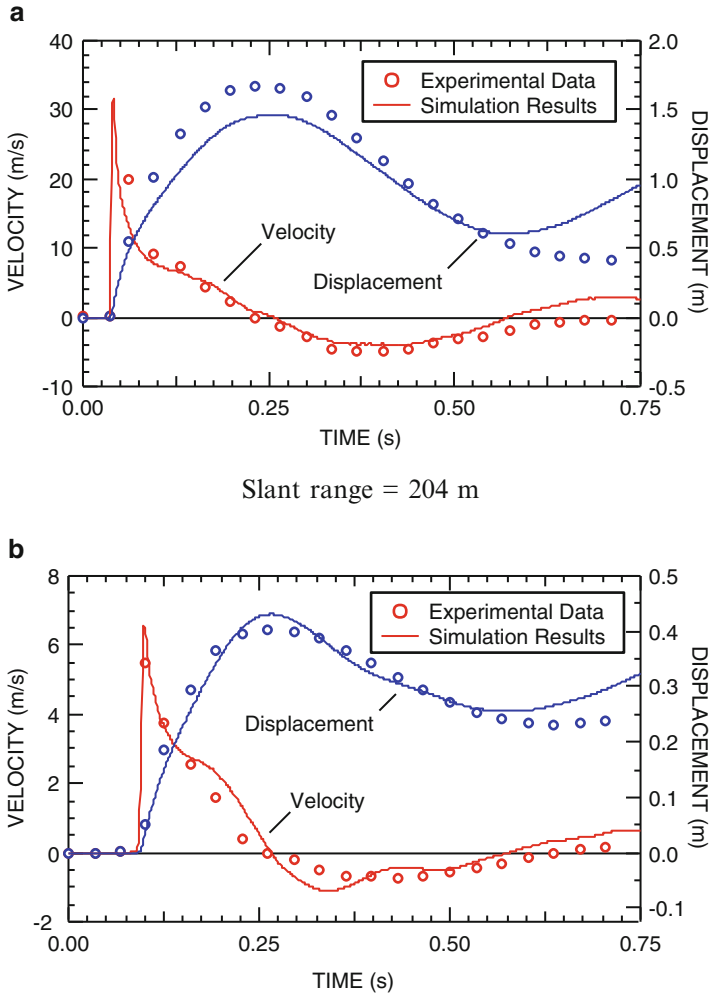


Fig. 2.2 Comparison of simulated and measured radial velocity and displacement histories at two different slant ranges away from the PILE DRIVER underground nuclear detonation

geologic medium during wave propagation, is reasonable when sufficient data are available to calibrate the model. When calibrated in this manner, the applicability of the model is limited to the geologic medium for which it was calibrated. Extrapolation to other locations where the joint spacing and/or orientation may be different from the original location will require recalibration of the constitutive model. This is illustrated in Fig. 2.4 which shows snapshots of the velocity field from two different 3D simulations of wave propagation in a jointed medium (Heuze and Morris 2007). The two snapshots on the left (Fig. 2.4a) correspond to a randomly jointed medium,

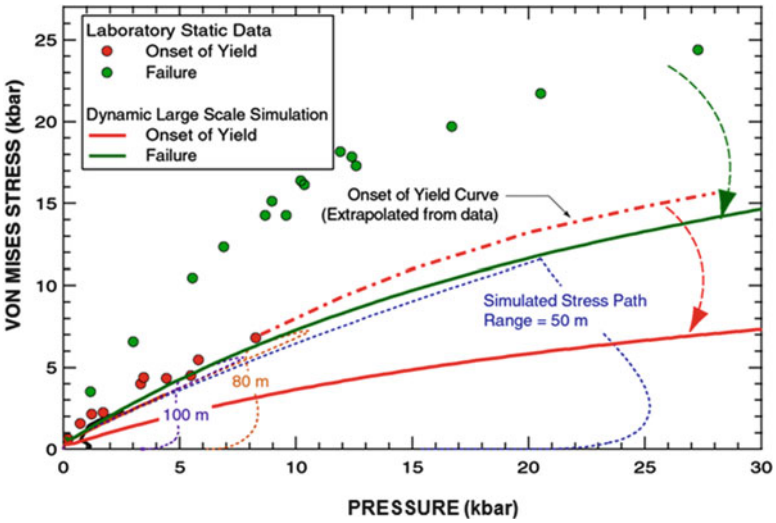


Fig. 2.3 Yield and failure surfaces for granodiorite used in the PILE DRIVER calculations (*solid curves*) together with the data from static experiments (Schock et al. 1973). *Dashed lines* are the stress path trajectories experienced by the material at different ranges away from the source of explosion

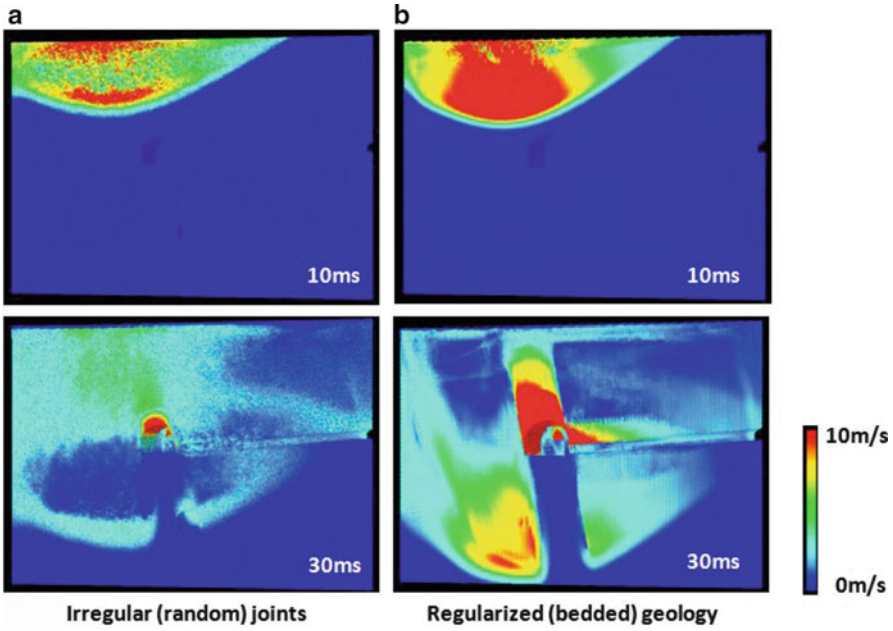


Fig. 2.4 Snapshots of the velocity field from two different LDEC simulations of wave propagation in a jointed geologic medium

while the snapshots on the right (Fig. 2.4b) correspond to a medium with bedding planes and regularized joints. Although the joint spacing and the contact properties used in the two calculations are the same, it is clear from Fig. 2.4 that joint orientation has a pronounced effect on the velocity distribution in the free field, and particularly in the vicinity of the tunnel. The constitutive model described above, which represents the state of the art in the groundshock modeling community, does not account for joint orientation and therefore is incapable of reproducing the kinds of effects shown in Fig. 2.4.

The currently used modeling approach is best described as "descriptive," and is distinguished from the sought-after "predictive" modeling approach wherein the effects of joints and other heterogeneities are taken into account using a rational physics based approach that relates the macroscopic continuum response of the medium to elemental properties like joint spacing, joint orientation, and interface properties. Recent advances in modeling capabilities coupled with modern high performance computing platforms enable physics-based simulations of jointed geologic media with unprecedented details, offering a prospect for significant advances in the state of the art. Initial steps demonstrating the feasibility of this approach have already been taken (e.g., Vorobiev et al. 2005; Vorobiev and Antoun 2011). As these novel approaches mature, they will be more tightly integrated in vulnerability assessment simulations thus reducing uncertainty in the simulation results and leading to more efficient and economical mitigation strategies.

Porous geologic materials present a unique set of challenges that must be addressed as part of a comprehensive constitutive model development strategy. Aside from the need for pressure–volume relations that take into account porous compaction and dilation, the question of saturation must also be addressed because under dynamic loading conditions, the response of dry porous geologic materials is markedly different from that of the saturated material. Furthermore, saturated soils, especially those with low cohesion, could undergo liquefaction, a phenomenon widely associated with structural damage during earthquakes. Liquefaction can also occur under shock loading conditions, leading to increased vulnerability and heightened risk of catastrophic structural failure.

Liquefaction occurs in loosely consolidated saturated soils when the shear resistance of the soil decreases as a result of increased pore pressure (or fluid pressure) during dynamic loading. Since the fluid only occupies the interstitial pore space, the pressure in the fluid increases in response to the decreasing volume brought about by porous compaction during loading. Under dynamic loading conditions like earthquakes and explosive applications, the rapid loading rate does not allow sufficient time for fluid migration to accommodate the transient increase in fluid pressure leading to an instantaneous loss of shear strength. This is accompanied by a transition from a solid-like response characterized by pressure-dependent strength to a liquid-like response governed by viscosity and hydrodynamic motion. Even if liquefaction does not occur, the decrease in strength associated with increased pore pressure in saturated geologic media during dynamic loading can have significant implications for the response of buried tunnels. Therefore, this effect must be incorporated in the constitutive model used to describe the behavior of the geologic medium in simulations of tunnel vulnerability.

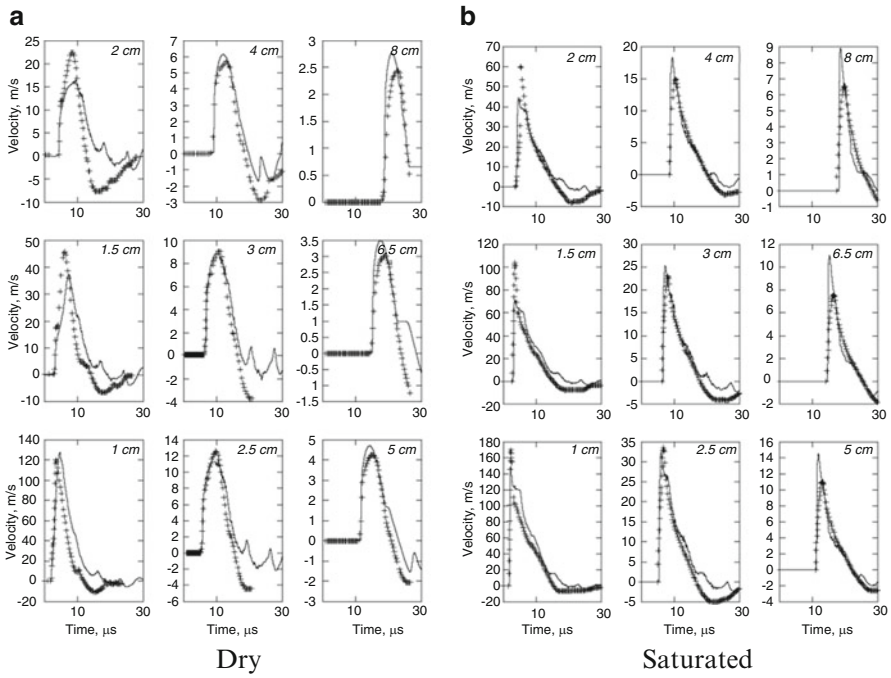


Fig. 2.5 Comparison of velocity waveforms for dry and saturated limestone at varying distances from the explosive charge. Experimental data (+) are from ref. (Gefken and Florence 1993) and simulation results (—) are from ref. (Liu et al. 2005)

The effective stress model, first introduced by Terzaghi for geotechnical applications, is used to account for the effect of saturation on the response of geologic media. This model has been used extensively to model the behavior of a variety of porous geologic materials including soils, concrete, and rock. In this formulation the "effective pressure" is introduced and defined as the difference between the total pressure and the fluid pressure (e.g., Jaeger and Cook 1976). The effective pressure is then used, instead of the total pressure, to determine the deformational and strength characteristics of the saturated material response.

The effective stress concept is particularly attractive because the saturated models can be trivially generated from the corresponding dry material models by providing a fluid equation of state. The model treats both fully and partially saturated materials and allows the use of arbitrary equations of state (from analytical equations, tabular data, or run-time databases) to be used for both the solid and the pore fluid. This is particularly useful at the high pressures associated with shock loading.

This effective stress model was used to simulate the behavior of porous limestone under shock loading (Liu et al. 2005). Experimental spherical wave data (Gefken and Florence 1993) for dry and saturated limestone were compared with results using the effective stress model. The model was first calibrated to fit the dry data as shown in Fig. 2.5a. The calibrated model was then used to predict the fully saturated response as shown in Fig. 2.5b. The significant differences in behavior between the

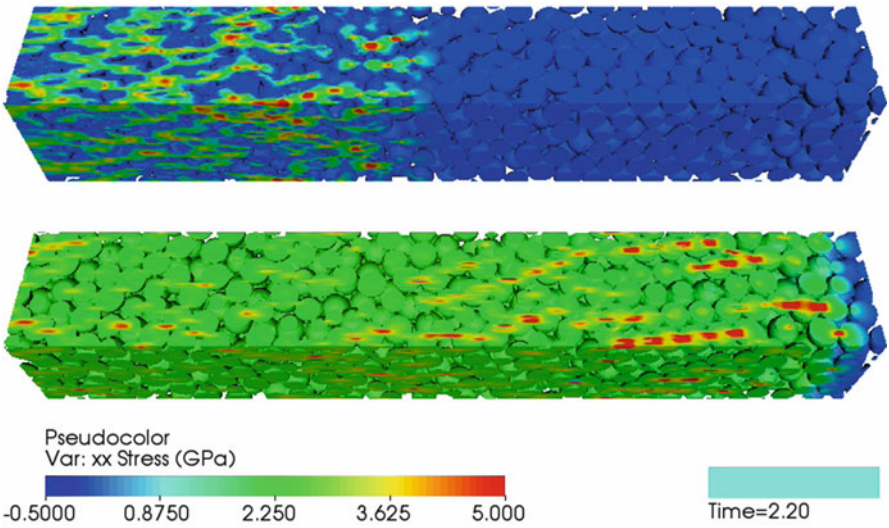


Fig. 2.6 Stress distribution in dry (*top*) and saturated (*bottom*) granular silica during shock loading. Significant differences in stress distribution and effective sound speeds are observed. The simulations were performed using GEODYN (2, Private Communication)

dry and saturated limestone are noteworthy. Also noteworthy is the fact that the effective stress model reproduces both the dry and saturated responses under shock loading with reasonable fidelity without changing any of the model parameters, thus demonstrating that the model can be reasonably expected to represent the behavior of variably saturated geologic materials in large scale simulations.

Terzaghi's effective stress model has been shown to work relatively well for most geotechnical applications, though significant deviations have been observed under pressures in excess of 100 MPa (Lade and de Boer 1997). These observations have also been corroborated with grain scale simulations (Fig. 2.6) of the response of representative volume elements of dry and saturated granular silica (SiO_2) (i.e., sand). At low pressures, the grain scale simulation results agree with the effective stress model predictions, but deviate significantly at high pressures. The development of improved modeling capabilities for saturated geologic materials is fertile ground for future research. An approach which combines grain scale simulations with experimental observations to elucidate the deformation mechanisms, leading to the development of a constitutive model that captures the main features of the material response, seems particularly promising and is being actively pursued.

2.2.3 Simulating Dynamic Structural Response

Dynamic simulations of the response of tunnels to explosive loading are complex multiphysics simulations that involve several nonlinear interacting phenomena with widely varying length and time scales. End to end vulnerability assessments often

utilize one or more multiphysics codes capable of representing the events and interactions of interest. Simulations using high-performance structural and fluid mechanics finite element codes are run on teraflop-class supercomputers to characterize structural response to explosive shock. Modeling frameworks of varying complexity are used to capture computationally demanding fully coupled soil-fluid–structure interactions. Explosive threats under different conditions of confinement or placement have been modeled using the ALE3D (Nichols and The ALE3D team 2009) and Paradyn (DeGroo et al. 2008) finite element codes, as well as discrete element and smoothed particle hydrodynamics (SPH) approaches (Morris and Johnson 2009).

Explicit structural dynamics codes like ParaDyn (DeGroo et al. 2008) are often used for system level response to structural failures, and multiphysics hydrodynamics codes like ALE3D (Nichols and The ALE3D team 2009) are used for fully coupled blast analysis. ParaDyn, the parallel version of DYNA3D (Lin 2005), is an explicit, transient dynamic analysis code for solid and structural mechanics which uses a Lagrangian formulation. Component failures can be accommodated through element erosion and the conversion of failed elements into SPH particles which preserve the system's mass and momentum balances. The SPH particles can interact with other particles and intact elements which provides a means to transfer the kinetic energy of failed components into other parts of the structure.

ALE3D is an arbitrary-Lagrangian–Eulerian hydrodynamic analysis code that simulates the fluid and elastic–plastic material response. The code incorporates continuum mechanics, thermal diffusion, chemistry, incompressible flow, multiphase flow, and magneto-hydrodynamics. The detonation energy released by the explosive can be represented using a JWL equation of state or other more complex models as described previously. The resulting shock wave is propagated through the surrounding medium (e.g., air, water, or a geologic medium) using advection and mesh relaxation techniques to allow material flow through the mesh without element tangling, which could compromise the quality of the numerical solution. The code tracks the wave propagation and interactions (reflections), so the blast pressures applied to the structure vary temporally (arrival time) and spatially (stand-off distance) as the blast wave travels over and around the structure. The materials representing the structure can be held Lagrangian to best preserve material history parameters or allowed to advect if severely deformed or extensively damaged.

Energy coupling into the structure often involves propagation of a blast wave either in air, in the case of an internal blast, or in water or a geologic medium, in the case of an external blast. Among the blast wave parameters of interest in assessing structural damage and tunnel vulnerability are peak material stress, positive phase impulse, and peak particle velocity. Resolving these quantities adequately in a hydrodynamic simulation places stringent requirements on the mesh size. Additional resolution requirements arise from the need to represent construction details (e.g., rebar in a reinforced concrete tunnel liner) that are likely to affect the dynamic response of the structure. Meeting these requirements necessitate a cell size on the order of 10^{-2} m. Additionally, problems of interest usually span spatial domains on the order of tens of meters in size. The three-dimensional multiphysics nature of the problem, coupled with the requirements for high resolution over large spatial domains lead to simulations that are of such size as to require the use of high

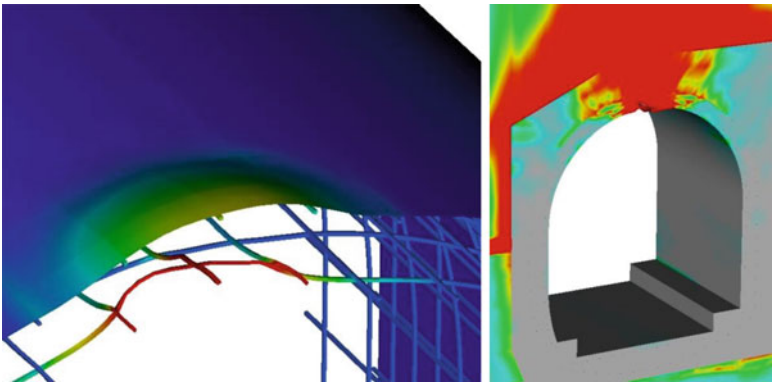


Fig. 2.7 High performance simulation of dynamic structural-failure of a complex soil/structure system; illustrated are the plastic strain of steel liner and rebar (*left*) and the material strain in soil and structure (*right*)

performance computing platforms to perform physically reasonable simulations in realistic wall clock time.

Several material models are available to represent the component materials' deviatoric strength and pressure–volume relationship (i.e., equation of state). Structural components can be modeled using a combination of beam, shell, and solid elements. Frame members (be they steel, iron, etc.) are often modeled using beam elements with user-defined integration rules to represent the joist, girder, and column cross-sections and account for partial yielding through a cross-section. The constitutive response is represented by large deformation inelastic models that include plasticity models with options for representing hardening, damage and effect of strain rate on material response. Concrete members are typically modeled with solid elements and often use the Karagozian & Case (K&C) concrete model (Malvar et al. 1997, 2000). The K&C model determines concrete strength with respect to confining pressure, damage, and strain rate. The K&C model also allows a homogenized representation of reinforcement using volume fractions. Dry and saturated geologic materials are modeled using the GEODYN material model as described in a previous section. Figure 2.7 shows a simulation of an underground reinforced concrete tunnel subjected to explosive loading. In this simulation, the tunnel structure was modeled with the K&C concrete model, the steel rebar within the concrete were modeled using an elastic–plastic model with a strain to failure criterion for rupture, and the saturated soil medium was represented using the GEODYN model with effective stress. As shown in the figure, the concrete tunnel experiences severe damage, including tensile rupture of several rebar, but the overall structural integrity of the tunnel is not compromised.

Structural damage is time-dependent and often requires several levels of analyses over different time-scales to determine the ultimate failure or survival of a structure. During an explosive event, structural damage in the form of a breach may be apparent within milliseconds after the blast and may be best modeled using specific fully

coupled codes such as described above and shown in Fig. 2.7. Longer term failure modes may be indirectly associated with a shock event and may occur at timescales on the order of seconds, e.g., longer term structural collapse, soil liquefaction, and the progressive collapse of a structure due to the failure of a critical support. Such longer term failure modes are likely to be realized by employing less computationally demanding capabilities that allow for longer temporal considerations.

Tunnel construction methods vary widely depending on the medium in which the tunnel is constructed and the intended function of the tunnel. Construction techniques vary from the reinforced concrete tunnel shown above, to cast iron and brick tunnels, to even unlined tunnels in competent rock where the strength of the rock is sufficient to maintain the stability of the rock mass. Assessing vulnerability of unlined tunnels presents a unique set of challenges which require highly specialized code capabilities to perform the analysis. As was previously discussed, rock masses are highly fractured, and those fractures have a controlling effect on wave propagation in the rock medium and on the response of structures buried therein. Assessing the stability of unlined tunnels therefore requires the utilization of a numerical method capable of explicitly accounting for the effect on joints (or fractures) on the response of the tunnel. Morris and Johnson (2009) developed the LDEC code specifically for performing this type of calculations. LDEC is a fully 3-dimensional, massively parallel code for simulating the stability of openings in fractured rock masses. LDEC represents the rock mass using a large number of polyhedral blocks that interact at their points of contact according to experimentally validated contact force laws. By directly simulating the discrete, blocky nature of rock masses, LDEC takes a fundamental approach to simulating the behavior of these systems while limiting the number of empirically derived model features.

LDEC was used to simulate the response of a tunnel complex to a near surface explosion in the vicinity of the tunnel (Morris 2004). The simulation was the largest of its kind and included a detailed facility spanning approximately 50 m with multiple tunnels and junctions. The fracture spacing in the rock was 30 cm, resulting in a computational domain of ~8 million polyhedral blocks and ~100 million computational elements. The facility was subjected to loading from a near-surface explosion, resulting in collapsed portions of the tunnels (Fig. 2.8). Simulations of the type shown in the figure are made even more daunting when geologic uncertainties are taken into account. In this case multiple runs are needed to assess the effect of variability in properties and rock texture (joint spacing and orientation) on the stability of the tunnel.

The closer a code is founded upon first principles of physics and chemistry (i.e., the less reliant on empirical calibration) the better the model is suited for problems of different scales and different applications. However, theoretical computational models can only approximate reality. Building confidence in the computational models requires extensive comparison to experimental data under loading and response regimes relevant to the application. Appropriate and carefully considered validation experiments can build confidence in the use of these computational tools. Ideally, validation experiments are true representations of the problem under consideration. This ideal is usually compromised: true experimental representations are costly or otherwise prohibitive, particularly when considering the importance of

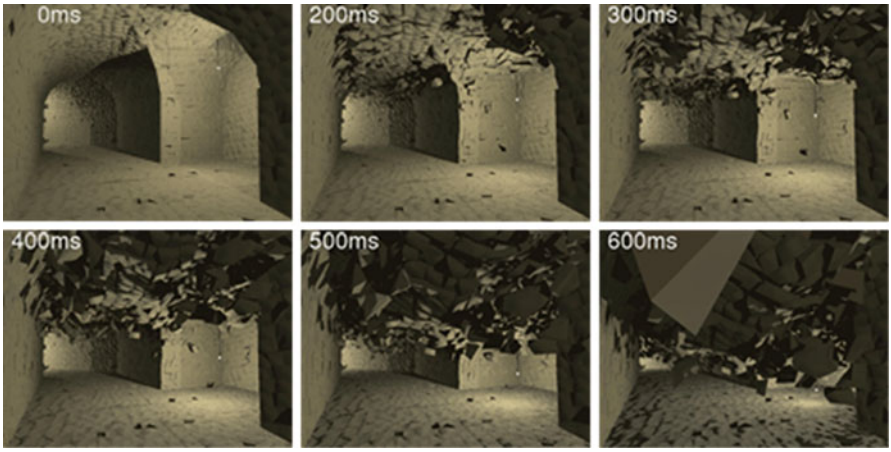


Fig. 2.8 Sequence of snapshots showing the progressive collapse of a section of a complex where an access drift intersect one of the main functional areas of the facility

experimental repeatability. Such is the case for structural systems of interest (tunnels, bridges, etc.) particularly when considering different failure modes spanning large timescales (e.g., blast failure taking milliseconds versus structural progressive collapse taking seconds to minutes to hours). Confidence in a model's ability to represent these large, and difficult-to-test, structural systems can be enhanced by carefully considered component tests, or by carefully and appropriately scaled phenomenological tests.

In building confidence in modeling the blast vulnerability of a large structural system, e.g., an aircraft fuselage or a tunnel structure, one must establish the level of detail necessary to answer the question at hand. For instance, if an order of magnitude threat-size is sufficient for making a decision, then less model validation will be required to establish model confidence, whereas other programs may require higher resolution of threat particularly if a threshold is important. The following items must then be considered in any study: (1) model construction and assumptions as well as parametric sensitivity, (2) verification of solution (model-to-model comparison or comparison to analytic solution is often sufficient here), and (3) a testing plan to validate models that can help provide metrics of confidence. A testing plan could include the following:

- Full-scale structure tests. These nearly "full system" tests are expensive, difficult to control and repeat, and may be prohibitive for structures of most interest, i.e., for a fleet of aircraft, or specific tunnels. Nonetheless, these types of tests are closest to the actual scenario of concern and highlight, at the very least, the primary mechanisms of system failure that must be captured, for instance, connection failure due to blast followed by the longer time progressive failure due to external loading. Any historical tests of this nature are valuable but limited in number. Full-scale tests are most effective if coordinated with numerical model analysts to optimize both the test design and to provide a set of tests that lend themselves best to model comparison.

- Component tests. These most basic component tests are relatively inexpensive and controllable providing confidence in the most fundamental aspect of modeling a structure under blast loads, for example, plate deflection and plate failure. Modifications of plates to represent structural complications, e.g., connections or rebar, can be included in a test to study specific failure modes. Careful consideration of plate testing must include the geometry of the plate relative to blast size as well as the influence of plate boundaries.
- Scaled bridging system tests. A scaled representation of the important structural components of a large structure could be a relatively inexpensive bridge between the small-scale component testing and the full-scale testing. Testing under loading conditions, for example at different pressurization levels, would build confidence in the ability of the models to capture consistently the relevant failure modes and timescales.

Following development of a validation process (test and modeling plan), impartial judgment by, e.g., a review board of experts or another independent organization with the relevant expertise, of the proposed process as well as the results is helpful. A difficulty, of course, is finding the right experts (expertise in blast-structure response is not commonly found) who are available to review the validation effort.

Verification and validation of the code and the models at the appropriate scale and under representative loading conditions are essential to ensure accuracy of the numerical results. Considerable efforts have been made to validate the blast responses predicted by these simulation tools. Figure 2.9 shows representative examples of the code benchmarking and validation efforts performed to increase confidence in the ability of the codes to reproduce important aspects of the experimental observations. Efforts such as the US Army Engineering Research and Development Center's Precision Test Wall Study, the Defense Threat Reduction Agency's Divine Buffalo and Discrete Gemini test series, and a host of smaller lab and field studies are used to partially validate simulations of air and underwater blasts. Such validation efforts also provide opportunity to evaluate the utility of, for example, faster running simplified approaches to structural response incorporating, for instance, homogenized material assumptions. Sample validation studies, illustrated in Fig. 2.9, include full-scale concrete testing (e.g., Crawford et al. 2004; Noble et al. 2005), and water-tamping/bubble-collapse testing (e.g., Thrun et al. 1993; Couch and Faux 1996).

Scale model testing can be an effective complement to large scale simulations in the assessment of structure vulnerability. Such an approach was taken by Glascoe et al. (2010) to evaluate a mitigation strategy for the protection of submerged structures from a standoff underwater explosion. Underwater explosions are efficient at the propagation of energy. Coupling the relatively high density with the relative incompressibility of water makes for enhanced shock transmission when compared to an air-blast of the same threat size (Cole 1948). For enclosed air-filled structures or ship hulls below the waterline, damage associated with shocks from a nearby underwater blast can be much more severe than damage associated with an air-blast from a similar sized threat.

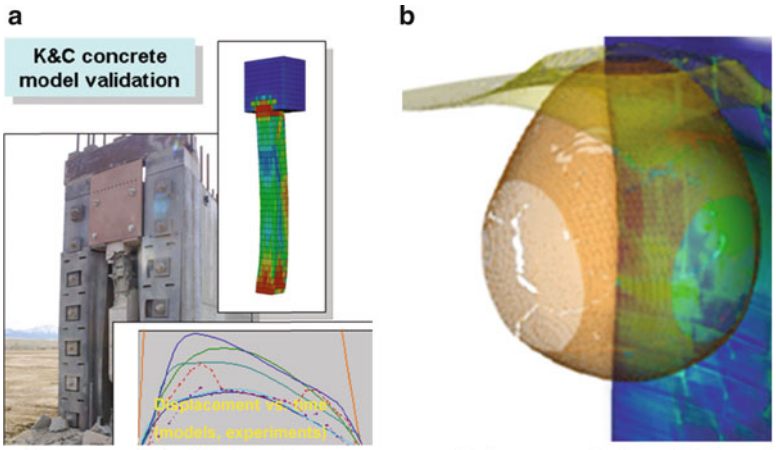


Fig. 2.9 Simulations of relevant experimental configurations are used to validate the codes and models used in numerical analysis of tunnel vulnerability

Effective mitigation of vulnerable structures against underwater shock is often best achieved by forcing increased standoff distance from the structure and by redistributing and/or breaking up the incident shock using strategically placed air pockets to maximize the impedance mismatch between materials, a function of density and sound speed. It is towards this end that the relative performance of a proposed mitigation option for a large concrete and steel structure was investigated: a belt of air-filled tubes encasing the waterside of an enclosed submerged structure.

A series of small (3-gallon) aquarium tests were used to evaluate the response of an instrumented aluminum plate to underwater explosions with and without mitigation near the charge. Several scaled 3-gallon aquarium experiments were designed including water-tamped tests without mitigation, water-tamped tests with mitigation, and an air-blast (control) test. A non-rupturing scenario was chosen for ease of model validation. The aquarium experiments were coupled closely with numerical simulation for pretest prediction and post-test comparison. The primary goal of the study is to couple the experimental results to numerical simulation for code validation and to build confidence in the proposed mitigation scheme. The ALE3D hydrodynamics code was used for experiment design, preexperiment deformation predictions, and post-experiment sensitivity studies.

The experiments were instrumented with a suite of diagnostic measurements that included pressure gages to measure the pressure history in the water, as well as strain gages and high speed photography to measure transient plate deformation during loading. Half of the aluminum plate was speckled for digital image correlation measurements. Figures 2.10 and 2.11 compare the temporal and full spatial field response of the aluminum plate's relative displacement from the DIC measurements. Figure 2.10 shows the response of the plate in the unmitigated test and Fig. 2.11 shows the response in the mitigated test. As shown in the figures, these measurements compare well with numerical predictions.

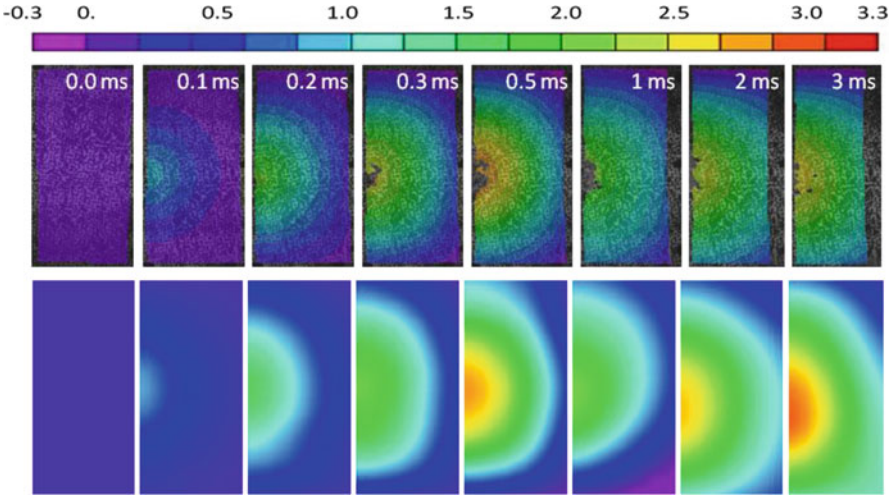


Fig. 2.10 Half-symmetry digital image correlation (DIC) experimental measurements in centimeters (*see color bar*) of relative plate deflection (*top images*) compare well with ALE3D simulation of plate deflection (*lower images*) for the unmitigated test over the first 3 ms

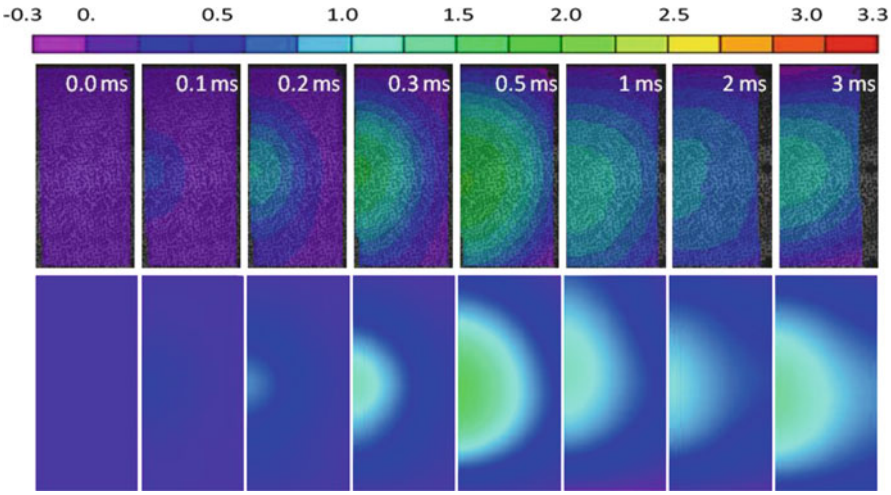


Fig. 2.11 Half-symmetry DIC plate deflection measurements (*top images*) in centimeters (*see color bar*) compare well with ALE3D simulation of plate deflection (*lower images*) for the mitigated test over the first 3 ms

Informed use of multiphysics modeling built upon experimental validation can form the basis of an end-to-end capability for analyzing and correcting structural vulnerabilities associated with explosive blast. These techniques are inherently computationally expensive due to the multi-dimensional nature of the problem space and the often necessary requirement for full coupling between fluid, solid and soil media phases. Computational expense can be minimized and results optimized

by use of simplified modeling approaches and by leveraging advanced stochastic sampling techniques. Such detailed but a timely analysis is particularly useful to accommodate the needs of government agencies and infrastructure owners to guide security efforts for critical infrastructure nationwide.

2.3 A Reduced Order Model for Tunnels: Pressure/Impulse Curves

Emergency response and national defense needs demand fast-running yet accurate tools as a first line of technical reachback and planning for both infrastructure protection and target defeat. Expert-constructed reduced order models (ROM) can form the basis for such tools. In this chapter, we discuss two types of tunnel ROMs that quickly and accurately simulate the blast environment and associated tunnel damage by portably leveraging high performance computing. The validated approach is robust, stable and lends itself to greater usability and interpretation by an engineer or scientist competent in explosives and structural response.

It is difficult to conduct direct simulation of blast propagation in tunnels or pipelines due to a combination of factors. Tunnels have high length to diameter ratios, resulting in a lengthy computational domain relative to tunnel diameter. Such long domains coupled with the high resolution required to capture the boundary effects that dominate the flow make direct three-dimensional simulation of flow in long tunnels prohibitively expensive. Even two-dimensional simulations of tunnels becomes computationally expensive when considering multi-parametric study and cannot be utilized if the tunnel system in question contains inherently three-dimensional features such as bends or intersections. One ROM that focuses on pressure and impulse (P/I) employs a simpler algorithm originally developed for gas guns (Glenn 1990, 1997) and captures the essential physics of blasts in tunnels (Glenn 2001; Neuscamman et al. 2011a, b), but runs in minutes on standard personal computing hardware. The approach taken for building this particular ROM for internal blasts in tunnels is described in detail below.

2.3.1 Building a Physics-Based P/I ROM

The P/I ROM for internal tunnel blast solves the one-dimensional fluid flow equations of mass, momentum and energy. The effects of wall drag are accounted for in the momentum equation using a friction factor, applicable to both laminar and turbulent flows. For simulation of an in-tunnel blast, the P/I ROM couples several one-dimensional representations of the tunnel and blast into a higher dimensional representation. Specifically, the code includes a spherical flow region for the detonation that is coupled to one-dimensional axial flow through the tunnel segments. By varying the cross section of the tunnel along its length, it is possible to account for the effect of platforms (larger cross section) and trains (restricted cross section)

upon the blast wave propagation and attenuation. The code can predict the effect of an arbitrary number of bends in a tunnel and supports coupling to additional one-dimensional segments to simulate the effect of tunnel intersections upon the shock wave. This ROM is ideally suited for providing pressure and impulse histories along a complex tunnel/station configuration to examine, for example, down-tunnel blast effects on personnel or impulse loading of structural components.

2.3.2 Validation of a P/I ROM

As discussed above, validation of any code is necessary before confident use. The P/I ROM has been validated against several sets of data involving a range of threat sizes and tunnel/pipe configurations (Glenn 2001). We compare the output of the P/I ROM to higher-fidelity two-dimensional axisymmetric hydrocode calculations using the ALE3D code as well as results from two small-scale high-explosive experiments done in Vicksburg at the now ERDC Laboratory.

Blast pressure data were obtained from a series of small-scale high explosive experiments of confined airblast (Lunderman and Ohrt 1997). In the experiment, a straight pipe section was simulated with a 243 mm inner diameter steel pipe (10 in. schedule 80 steel pipe). Pipe sections were connected with heavy bolted flanges to form an assembled tunnel about 7.75 m in length. The inlet was constructed with steel plates to emulate the entrance to a real tunnel in a mountainside. The far end of the pipe was left open. Pressure profiles were obtained using diaphragm-type air blast gages flush-mounted to the wall of the pipe. Spherical explosive charges were formed from hand-packed hemispheres of composition C-4. The hemispheres were packed around a detonator to approximate a center-detonated charge. The charge was suspended by the firing line of the detonator to the centerline of the pipe. A series of detonations were conducted, with varying charge size and location. We focused on the 15.7 g C-4 charge located inside the pipe, four pipe diameters (D) from the inlet. This configuration was simulated with the two codes assuming rigid walls and the ALE3D simulation calculating the 2D axisymmetric solution.

Peak pressure and impulse results from each simulation and the experiment are shown in Fig. 2.12. Both simulations show good agreement with the experimental data. The STUN calculation performs better than ALE3D for this metric, and agreement to experiment increases for peak pressure at x/D locations greater than one. Very close to the explosive source, both models under-predict the peak pressure measured in the experiment. However, further downpipe, when the flow has developed into normal shock wave propagation, we see excellent agreement. ALE3D peak pressure results also improve with distance down the pipe, but impulse is consistently under-predicted. Full pressure and impulse profiles at 15.7 diameters down the tunnel are shown in Fig. 2.12; the STUN profiles at this measurement position are virtually congruent with the experimental ones.

The second set of simulations compares to data from an experiment involving an explosion in a steel pipe where the blast wave encounters a sudden decrease in cross-section (Lunderman et al. 1993). In this case, a 340 g charge of C-4 explosive

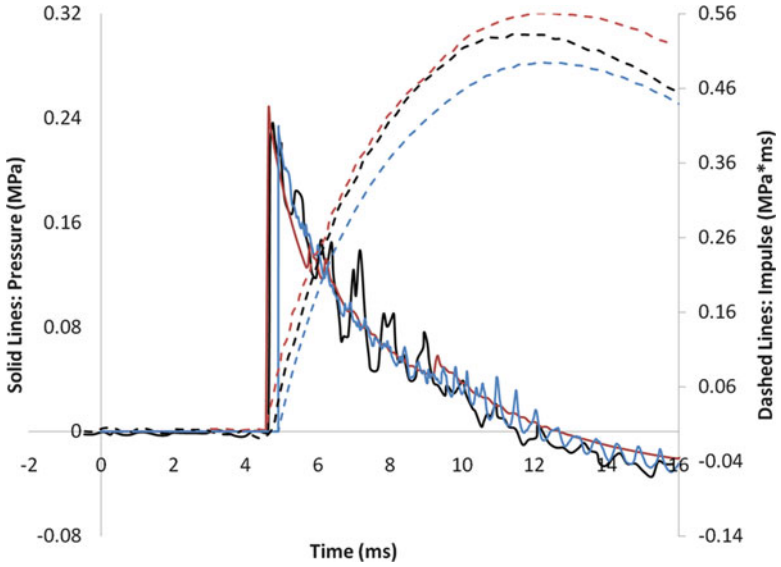


Fig. 2.12 Peak pressure (*left axes*) and impulse (*right axes*) comparison of 1D ROM prediction (*red lines*), a 2D hydrocode prediction (*blue lines*) and the experiment of Lunderman and Ohrt (*black lines*)

(5.04 cm × 5.04 cm × 8.23 cm) was centered in a 1.8 m long section of heavy duty steel pipe with an internal diameter of 14.6 cm (the detonation chamber). Connected to one side of the detonation chamber were a set of 4 m long segments of smooth Schedule 80 steel pipe with an internal diameter of 7.36 cm. On the other side, a similar arrangement was used except that the center two segments were replaced by grooved pipe. Pressure profiles were obtained using diaphragm-type air blast gages flush-mounted to the wall of the pipe; no pressure gages were used in the detonation chamber. For the purposes of this study, the focus is on the smooth side and the fourfold decrease in cross section that occurs at the end of the detonation chamber. The experimental setup was again simulated assuming rigid walls with the ROM and ALE3D codes, and the ALE3D simulation ran in 2D. The numerical results from both codes are in good agreement in terms of both pressure and impulse (Fig. 2.13).

The reduced order physics code for estimating blast effects in pipelines or tunnels performs exceptionally well when comparing to experimental data for a smooth, straight pipe. Down tunnel from a contraction, STUN overestimated peak pressure and impulse compared to both the experiment and 2D axisymmetric ALE3D simulation. However, since the goal is to create a fast-running tool, the relative calculation times should be considered. The 1D calculation in each study was carried out on a single processor PC in less than a minute of clock time whereas the 2D calculations required 2,300 h (96 h on 24 processors) for the single pipe simulation and 18 h (6 h of clock time with 3 processors) for the two pipe with a contraction simulation.

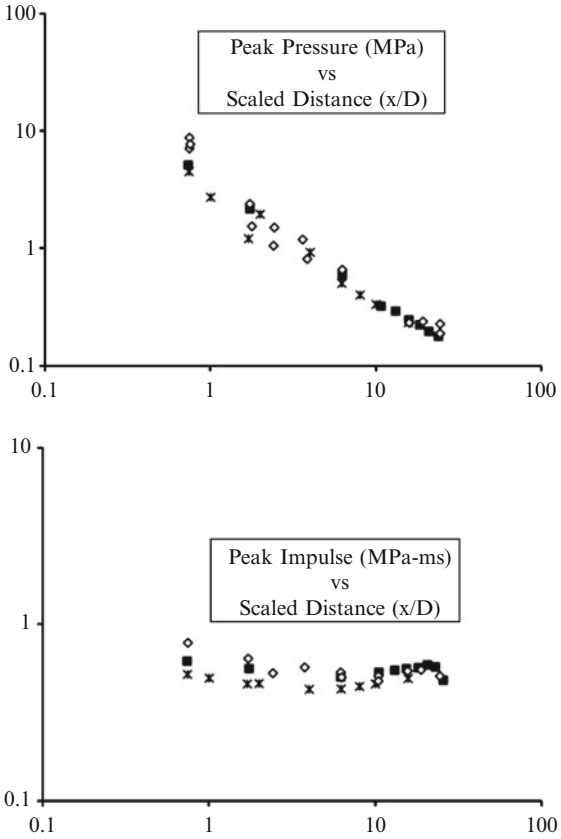


Fig. 2.13 Modeled peak pressure and impulse (*top and bottom plots*) by the 1D ROM (*filled square*), the 2D hydrocode (*open circle*), and experimental results (*multiplication sign*)

2.3.3 P/I ROM Example: An Explosive in a Complex Tunnel System

An example of a complex hypothetical single tunnel system is useful for illustrating the utility of the P/I ROM for tunnels. Figure 2.14 illustrates a tunnel with a 1,000 m straight section running to the left of the explosive source and a complex system of partial blockages (contractions), expansions, and multiple drifts to the right of the explosive source. The black dots indicate points where time varying details of pressure and impulse per unit area can be acquired after simulation. This particular example is computed quickly (tens of seconds on a 2012 single processor laptop) producing both pressure and impulse per unit area histories at various locations. Figure 2.15 illustrates peak overpressure as a function of distance from the charge both down the straight section (left) and the complex section (right). Peak pressure observed across the tunnel is useful information when considering life-safety in a tunnel away from a blast, or when considering the design of secondary structures in

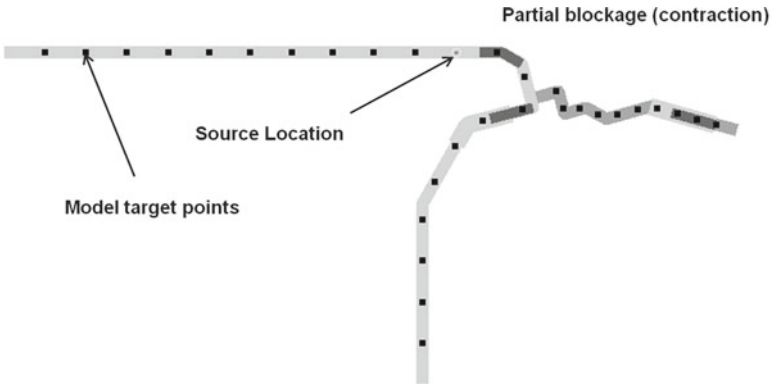


Fig. 2.14 A hypothetical complex tunnel system is constructed to illustrate an example use of the P/I ROM. Shown here is a tunnel with a 1,000 m "straight tunnel" running to the left of the explosive source and a "complex tunnel" system of partial blockages (contractions), expansions, and multiple drifts to the right of the explosive source

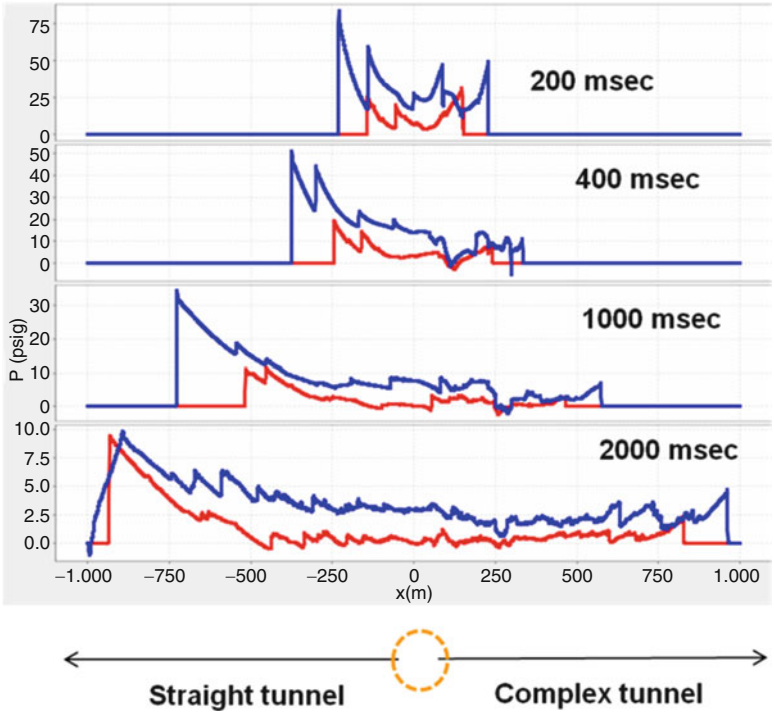


Fig. 2.15 Pressure profiles in time propagating down the left-hand "straight tunnel" and right-hand "complex tunnel" of Fig. 2.14

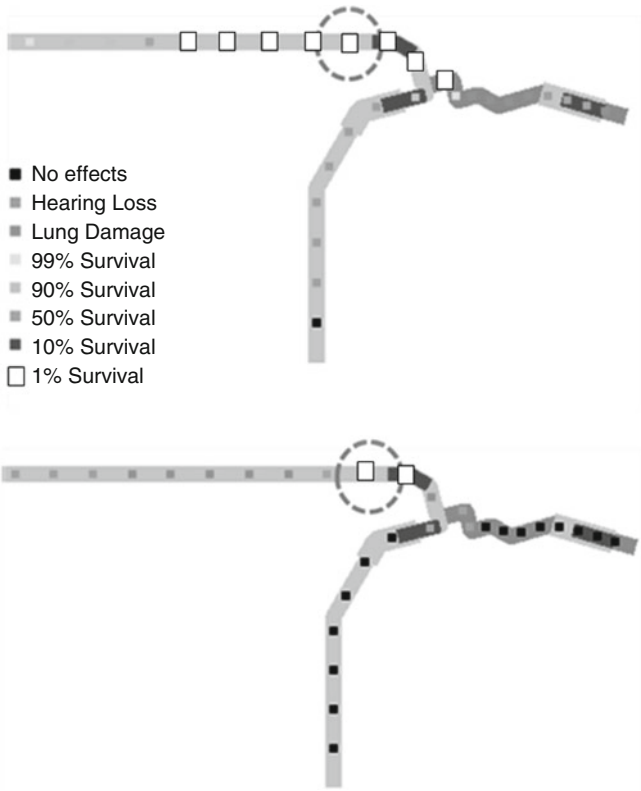


Fig. 2.16 Down-tunnel blast effects on people using P/I fragility curves on scenarios of the system in Fig. 2.14; shown are the effects of a large explosive (*top*) and a small explosive (*bottom*). Results are illustrated on a point by point basis for output purposes only

a tunnel system (e.g., emergency lighting, ventilation structures). It is notable that the pressures could be significantly higher if the explosion were tamped by the presence of a train or other large object located near the charge.

The severity and extent of personnel injuries along the tunnel, as well as in the stations and drifts, can be estimated by using fragility curves of Bowen et al. (1968) relating human survivability to the peak overpressure and duration of exposure to the blast overpressure as plotted in Fig. 2.16. Survivability estimates are evaluated at the same target points specified for the pressure time histories (refer to Fig. 2.14). The target points are gray-scale coded according to the survival probability. In this example, the blast overpressures have dropped below the threshold for 1 % survival in the complex section of the tunnel (right) sooner than in the straight section of the tunnel (left) for both a large and a small explosive. Such information can be used in conjunction with system usage data to estimate the number of casualties that might occur for a particular scenario to assist stakeholders in response planning.

2.4 A Reduced Order Model for Structures: Complex Failure

The simplified physics code discussed above allows tool users to determine the characteristics of the blast propagation along a tunnel; however, a fully 3D calculation is required to estimate near field damage, e.g., structural failure, for a given threat and tunnel configuration and these calculations cannot be accommodated in fast-running mode. Accordingly, we have used a statistical learning approach to deal with this problem. Using ALE3D, a series of parametric calculations was performed to identify bounds on the values of charge size, standoff distance, and wall thickness that may result in structural breach. First, a high fidelity multiphysics model of a generic but representative structure is created that can be run and rerun under different threat and tunnel conditions. Careful consideration of the trends gleaned from these runs can be used to generalize multi-parameter "response curves" for rapid assessment (Fig. 2.17).

2.4.1 Building a Complex Failure ROM: HPC Response Analysis

Numerical analyses are conducted for a hypothetical steel- (rebar) reinforced concrete tunnel or pipe system of limited length. Constrained boundary conditions are imposed at the bottom of the soil surrounding the tunnel, the side boundary, and the

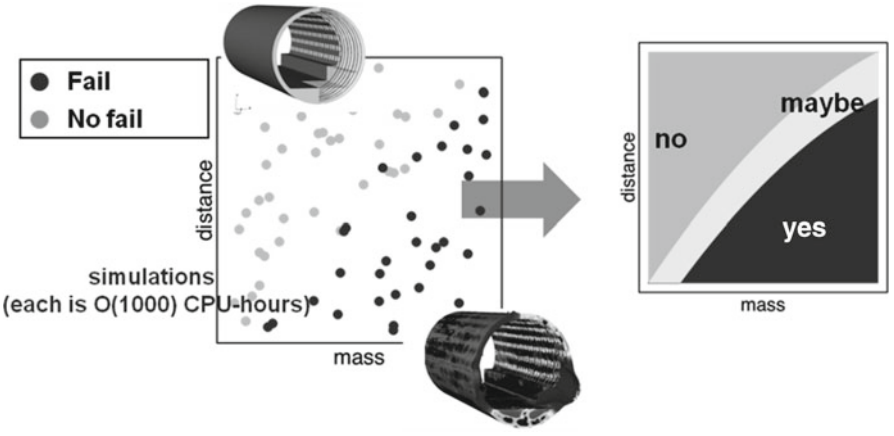


Fig. 2.17 Careful deliberate selection of high fidelity calculations of a full three-dimensional soil/fluid/structure blast calculation can be used to create an interpolated lookup of a specific mode of structural response (in this case "breach") under a range of variable conditions, e.g., variable charge mass and charge standoff distance

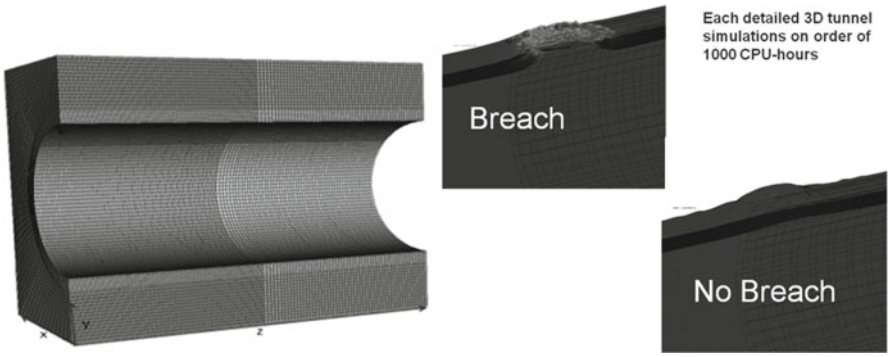


Fig. 2.18 An example of a breached concrete structure; the breached zone is defined by a dual criteria capturing tensile and compressive failure. Note that this figure shows "breach" by removing elements considered to be failed by our dual criteria

vertical section of soil and concrete portion where nodal velocities are assumed to be near zero. Continuous pressure boundary and zero fluxes of energy and mass are assumed for the vertical face of the air portion within the structure's inner radius. The center of the spherical charge is located, and its radius is calculated, based on the standoff, charge weight and fixed density of charge. Standoff is defined as the distance from the tunnel wall to the closest point on the charge's surface. Structural damage is quantified using a combined index of shear dilation and density change in the concrete. Both metrics indicate the separation of aggregate and mortar necessary for the formation of rubble.

Damage evaluation must take place in two steps because the continuum representation of the structure is incapable of developing a breach hole. Elements that begin the simulation connected must remain so throughout the duration of the simulation. To determine breach, a description must be made of the portions of the concrete material, if any, that have sustained heavy damage (Fig. 2.18). Information must be extracted from the phenomenological plasticity model to determine damaged sections. First, portions of the structure that have been determined to contain rubble are highlighted. Compressive damage is tracked well by material dilation. Dilation is a natural and observed phenomenon in actual concrete and other geological materials that occur when the concrete is experiencing shear stress and aggregate begins to "roll over" the neighboring particles. Large dilation strains emulate a real-world loading scenario where aggregate has been separated violently from the mortar. Based on Split Hopkinson pressure bar tests and expert analysis, a 0.85 % volumetric strain *from dilation* is chosen to represent damage (see Fig. 2.19). Another indication of concrete damage severe enough to cause breach is a decrease in density which can be similarly compared to dynamic Brazilian split cylinder tests (Fig. 2.20). Density is tracked by the constitutive material model and its decrease can be attributed to cracking and spall failure.

Next, the calculated breached volumes based on the dilation and density results are inspected by an analyst to see if they are likely, in his or her opinion, to

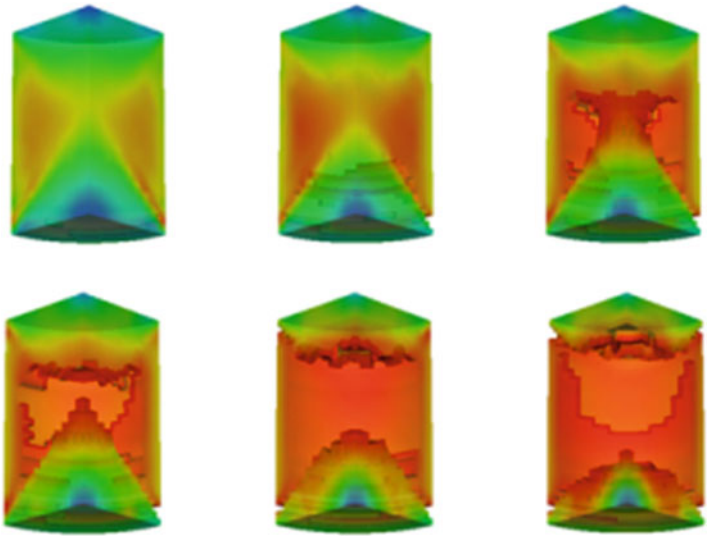


Fig. 2.19 For breach determination, split-Hopkinson pressure bar (SHPB) tests were modeled for dilation and rubble formation; shown are modeled SHPB concrete specimens in quarter symmetry and the evolution of modeled failure cones from top left to bottom right under ever increasing strain rate. Note with increasing strain, failure cones begin to form illustrating a dilation failure model represented in the breach

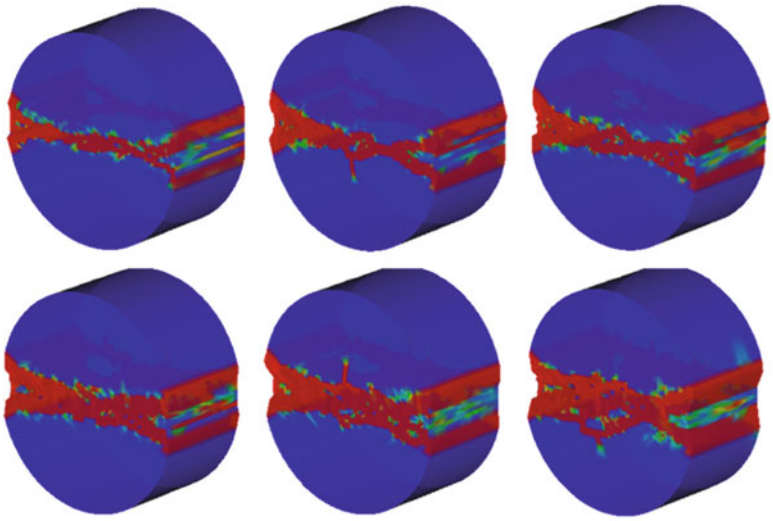


Fig. 2.20 Breach criteria for damage in tension can be represented as a density drop and compared to dynamic "Brazilian" split cylinder tests. Shown here starting from top left moving to bottom right is a modeled decrease in density (*lighter portions*) for a concrete sample under a direct side impact of the specimen representing the split cylinder test

constitute a breach. Finally, the analyst's decisions about breach, which include an option for indeterminate or "possible breach," are fed into a statistical algorithm that produces breach curves, as described in the following section.

2.4.2 Building a Complex Failure ROM: Statistical Emulation

Due to the high computational cost, breach determination via the full 3D physics model is not feasible for every structure/charge configuration of interest. Statistical emulation can be used to supplement a limited number of model runs and provide breach predictions for the full parameter space. Such emulators can also be used as a part of an adaptive sampling strategy, to ensure that costly 3D simulations are run only at points with high predictive value. Once we have adequately characterized the parameter space through such adaptive sampling, we use our emulator to generate "breach curves" as shown in Fig. 2.22. These curves, generated from a relatively small number of precomputed simulation runs, are included in our fast-running tool, and can provide users with breach risk assessments for a wide variety of threats almost instantly.

A support vector machine (SVM) is a classifier that generalizes a maximal margin hyper plane: the linear surface that divides two classes with the largest "margin" from existing data. Only a few points (support vectors) define the classification boundary. The SVM extends this framework to nonlinear boundaries by using kernel functions to map data into a higher dimensional space, and by introducing slack variables to allow for classification errors. SVMs can be used for adaptive sampling. Choosing new points which lie along the current boundary will maximize the information gained. This is critical for computer experiments, where sampling may be costly.

Our methodology was developed to address several challenges inherent, and in some cases unique, to our breach prediction problem: a priori constraints on our decision boundary, uncertainty in breach classification, and the need for adaptive sampling. Our first constraint relates to the need to incorporate knowledge of breach behavior into our classifier. In particular, our classifier needed to exhibit proper monotone behavior (increasing charge weight increases risk, increasing wall thickness decreases risk, etc.) and the fact that there is no risk of breach below a known threshold value. We also had to address the uncertainty in breach characterization. Recall that, in addition to simulation runs that clearly failed or clearly did not, there were a number of "possible breach" cases. Finally, we needed a method that had the ability to improve its own results through adaptive sampling. While we began this stage of the project with several hundred existing simulation runs, they were not necessarily in the neighborhood where the boundary for our final breach criterion would be. Therefore, we needed a way to identify "high value" points for new simulation runs, which would allow us to further refine our classifier.

All of these factors lead to the decision to use parametric support vector machines (PSVMs; Lennox and Glascoe 2011). The PSVM is a form of the standard support vector machine (Cortes and Vapnik 1995) that allows the form of the classification boundary to be constrained by expert knowledge (Fig. 2.21).

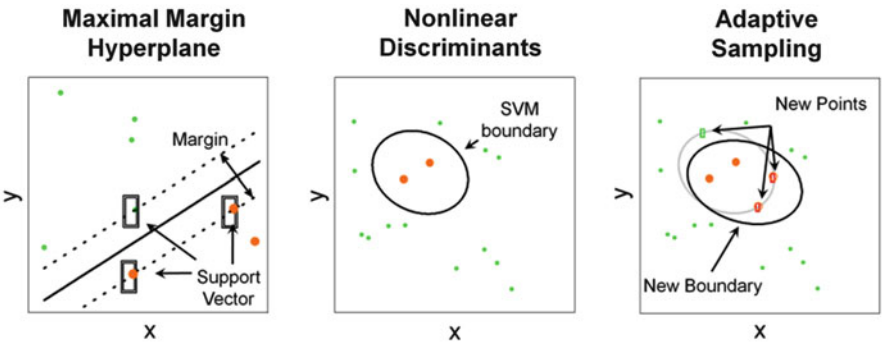


Fig. 2.21 Support vector machine approach with adaptive sampling

Our problem involves three classes: breach (also referred to as "red" for the color used in the breach curve in our tool), no breach (green), and possible breach (yellow). We define the yellow region by fitting two separate classifiers. The first classifier combined all possible breach points with no breach points, and constituted the boundary between red and yellow areas on our plots. The second made the more conservative assumption that all possible breaches should be counted as breaches, and this classifier was used to generate the green/yellow boundary. As is typical for active learning with SVMs (Basudhar and Missoum 2008), our strategy focuses on selecting points on these classification boundaries.

To select a new set of test points for boundary refinement we generated a candidate set of points located on either the conservative (green/yellow) or anti-conservative (yellow/red) SVM boundary. For every point in the candidate set, we determined the closest neighbor in the current data, and the distance to this closest neighbor. The point with the maximum distance from its nearest neighbor ("maximin" criterion) was chosen to be added to the dataset, see Fig. 2.22 (right plot). All variables were scaled to fall between zero and one to ensure that those with the largest ranges did not dominate this point selection process. The process was then repeated for the remaining candidates, until we found a reasonable test set size (on the order of 25–50 points), and then these were processed using our ALE3D model. The new points were then added into the dataset, new SVM boundaries were calculated, and the adaptive sampling process repeated (Fig. 2.23). The finalized breach curves are accessed through the same user interface as the 1D model and take a form similar to Fig. 2.22.

2.4.3 A Failure ROM Example: With and Without Liner Mitigation

An example of a hypothetically failing structure is useful for illustrating the utility of a structural failure ROM. Here we consider two sets of hypothetical reinforced

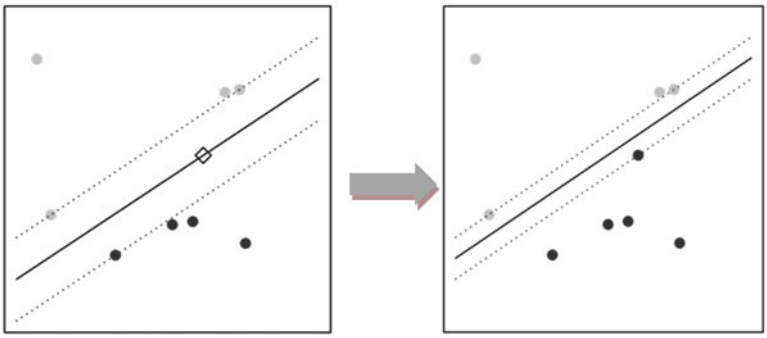


Fig. 2.22 Notional standoff versus threat size breach curve (*left plot*). The *right plot* shows a linear SVM separating two classes. The *diamond* represents a highly informative point (located on the decision boundary and distant from existing points) that would be selected by our adaptive sampling method for evaluation

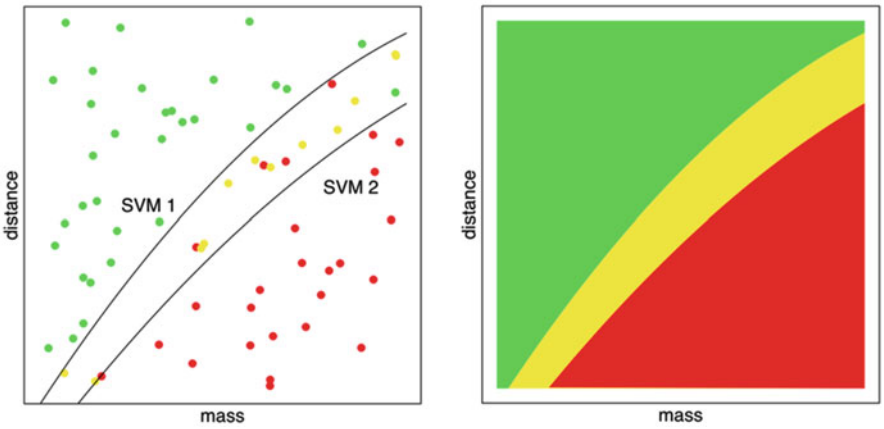


Fig. 2.23 Structural response output in terms of breach (*red*), no breach (*green*), and indeterminate (*yellow*). *Left* is a plot of the discrete three-dimensional output and the use of sequential vector machine (SVM) curves separating no breach (SVM 1) and separating breach (SVM 2). The resulting continuum shown *right* is used as output to the fast running tool

concrete structures with and without a ¼″ thick steel plate on the outside part of the structure. Breach is considered if the structure "daylights" after the modeled explosive event, i.e., a clear hole exists through both concrete and plate. The response curves discussed in the subsection above are employed and generated using the SVM methodology; two SVMs segregate the breach into likely breach, possible breach, and unlikely breach. The two sets of response curves in terms of standoff and threat size are illustrated for a baseline concrete structure (Fig. 2.24) and for a structure of twice the concrete thickness (Fig. 2.25). All results are expectedly

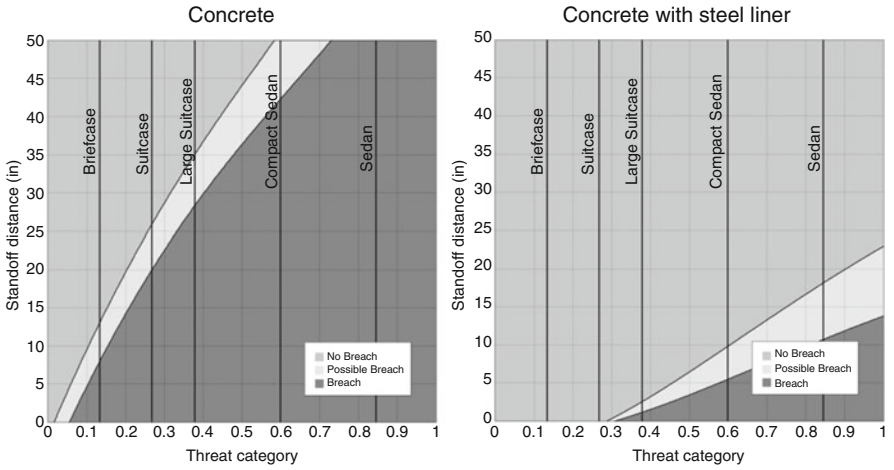


Fig. 2.24 A hypothetical reinforced concrete structure as represented by the complex failure ROM. On the *left* is the structure without an external steel liner; on the *right* is the structure with a ¼″ thick steel liner

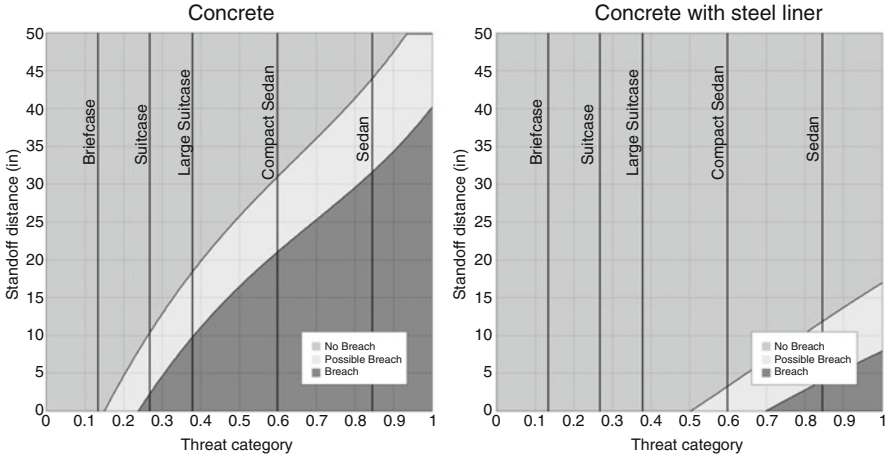


Fig. 2.25 A hypothetical reinforced concrete structure twice as thick as the structure in Fig. 2.24. On the *left* is the structure without an external steel liner; on the *right* is the structure with a ¼″ thick steel liner

monotonic with respect to breach failure and standoff and threat size. The thick concrete structure requires a much larger charge at, for example, 25 in. of standoff (a vehicle bomb) than the thinner concrete structure (a suitcase bomb). The efficacy of the steel mitigation is obvious: neither structure is likely to be breached at 25 in. of standoff if a ¼″ steel liner is present.

2.5 Summary

High performance computational hydrodynamic and structural analysis tools are useful for predicting the response of structures to impulsive dynamic loads, assisting in the implementation of vulnerability corrective measures to reduce overall risk. As these tools require significant computational resources, timely assessment involving a large range of threats and threat locations is difficult. Consequently, there is a need for capabilities that can rapidly evaluate effects associated with various threat sizes, threat locations, and system states while quickly highlighting uncertainties associated with structural and system response. In this chapter we highlighted the importance for high fidelity models of tunnels with considerations of the energetic source of the shock, the physics of geologic response to strong dynamic loads, and, ultimately, the physics of structural and material response and failure resulting from dynamic shock loading events. Careful validation of these high fidelity tools is necessary to provide confidence in model prediction. Faster running, phenomena-focused, reduced order models can be constructed from these validated higher fidelity capabilities to quickly estimate the effects of explosions within a contiguous system of confined spaces such as tunnels. Emergency response and national defense needs demand fast-running yet accurate tools as a first line of technical reachback and planning for both infrastructure protection and target defeat. Expertly constructed reduced order models can form the basis of such tools whether the simplification is by using a 1D limited physics code instead of a 3D code when assumptions permit, or by providing a response curve fitted to previously analyzed high fidelity multiphysics analysis.

Acknowledgments This work is performed under the auspices of the US Department of Energy by Lawrence Livermore National Laboratory under Contract DE-AC52-07NA27344. We would like to thank the Department of Homeland Security (DHS) Science and Technology (S&T) Directorate and the Transportation Security Administration for their sponsorship and assistance in these efforts. We particularly acknowledge the assistance and leadership of Dr. John Fortune (S&T), Dr. Mary Ellen Hynes (S&T), and Mr. Christopher McKay (TSA). We would also like to acknowledge the technical contributions of Lew Glenn, Larry McMichael, Chad Noble, Ilya Lomov, Stephanie Neuscamman, Oleg Vorobiev, Joe Morris, Greg Schebler, Allen Kuhl, Ben Liu, Ed Kokko, Ana Kupresanin, and Will Elmer. This document is LLNL-BOOK-589112.

References

Antoun TH, Vorobiev OY, Lomov IN, Glenn LA (1999) Numerical simulations of an underground explosion in granite. 11th topical conference on shock compression of condensed matter, Snowbird, UT, June 27–July 2, 1999

Antoun TH, Lomov IN, Glenn LA (2001) Development and application of a strength and damage model for rock under dynamic loading. In: Elsworth D, Tinucci J, Heasley K (eds) Proceedings of the 38th U.S. rock mechanics symposium, Rock mechanics in the national interest. A.A. Balkema, Lisse, The Netherlands, pp 369–374

Basudhar A, Missoum S (2008) Adaptive explicit decision functions for probabilistic design and optimization using support vector machines. Comput Struct 86(19–20):1904–1917

Bowen LG, Fletcher ER, Richmond DR (1968) Estimate of man's tolerance to the direct effects of air blast, Defense Atomic Support Agency Report DASA-2113
Cole H (1948) Underwater explosions. Princeton University Press, Princeton, NJ
Cortes C, Vapnik V (1995) Support-vector networks. Mach Learn 20:273–297
Couch R, Faux D (1996) Simulation of underwater explosion benchmark experiments with ALE3D. Lawrence Livermore National Laboratory, UCRL-CR-123819, 1996
Cowperthwaite M, Zwisler W (1974) TIGER computer program documentation. Stanford Research Institute Technical Report, AD/A-02 791, March 1974
Crawford, Malvar JL, Shi Y (2004) Verification and validation for DYNA3D models of RC components subjected to cased and uncased munitions. Karagozian & Case, TR-99-10.3, October 26, 2004
DeGroo A, Sherwood R, Hoover C (2008) ParaDyn, a parallel nonlinear explicit, three-dimensional finite element code for solid and structural mechanics. Version 8.1 user manual, LLNL-SM-407000, Lawrence Livermore National Laboratory
Fried L (1995) CHEETAH 1.22 user's manual. Lawrence Livermore National Laboratory, Livermore, CA, UCRL-MA-117541, Rev. 2
Gefken PR, Florence AL (1993) Spherical waves in jointed limestone. SRI International, Defense Nuclear Agency Report No. DNA-TR-92-122
Glascoe L, Noble C, Reynolds JG, Kuhl A, Morris J (2009) Securing transportation systems from high explosive threats. Proceedings of the 2009 IEEE international conference on technologies for homeland security, Waltham, MA, LLNL-PROC-411500, May 11–12, 2009
Glascoe L, McMichael L, Vandersall K, Margraf J (2010) Underwater blast experiments and modeling for shock mitigation. 14th Det Symposium
Glascoe L, Elmer W, Glenn L, Kupresanin A, McMichael L, Minkoff S (2011) Proceedings for DHS University summit, Washington, DC, 7 February
Glenn LA (1990) Design limitations on ultra-high velocity projectile launchers. Int J Impact Eng 10:185
Glenn LA (1997) On how to make the fastest gun in the West. Proceedings of the international workshop on new models and numerical codes for shock wave processes in condensed media, St. Catherine's College, Oxford, UK, September 15–19, 1997
Glenn LA (2001) Simulating MARVEL with the STUN Code. LLNL UCRL-ID-143993, June 6, 2001
Heuze F, Morris J (2007) Insights into ground shock in jointed rocks and the response of structures there-in. Int J Rock Mech Min Sci 44:647–676
Hoek E (1994) Strength of rock and rock masses. ISRM News J 2(2):4–16
Hoek E, Brown ET (1980) Underground excavations in rock. The Institution of Mining and Metallurgy, London
Jaeger JC, Cook NGW (1976) Fundamentals of rock mechanics. Halsted, New York
Lade PV, de Boer R (1997) The concept of effective stress for soil, concrete and rock. Géotechnique 47:61
Lawrence Livermore National Laboratory (2012) LLNL explosives reference guide, Lawrence Livermore National Laboratory, online limited access website, October 2012
Lee E, Tarver C (1980) Phenomenological model of shock initiation in heterogeneous explosives. Phys Fluids 23:2362–2372
Lee E, Hornig H, Kury J (1968) Adiabatic expansion of high explosive detonation products, UCRL 50422, Lawrence Livermore Laboratory, May 1968
Lennox KP, Glascoe L (2011) Constrained classification for infrastructure threat assessment. In: Proceedings for the IEEE international conference on technologies for homeland security, 15–17 November, Waltham, MA
Lin J (2005) DYNA3D: a nonlinear, explicit, three-dimensional finite element code for solid and structural mechanics user's manual. UCRL-MA-107254
Liu BT, Lomov I, Vorobiev O (2005) Simulation of shock loading in saturated geologic materials. In: Khan AS, Khoei AR (eds) Dislocations, plasticity, damage and metal forming: material

response and multiscale modeling. Proceedings of plasticity '05: the 11th annual symposium on plasticity and its current applications. NEAT, Fulton, Maryland, pp 346–348
Lomov I, Pember R, Greenough, Liu B (2005) Patch-based adaptive mesh refinement for multi-material hydrodynamics. In: Five-Laboratory Conference on Computational Mathematics, Vienna, 2005
Lunderman C, Ohrt AP (1997) Small-scale experiments of in-tunnel airblast from internal and external detonations. 8th International symposium on interactions of the effects of munitions with structures, April 21–25, McLean, Virginia
Lunderman CV, Welch CR, Joachim CE, Furey JS (1993) Effects of tunnel wall roughness on airblast from internal detonations – results from small-scale experiments. 64th Shock & vibration symposium, October 25–28, Fort Walton Beach, Florida
Malvar L, Crawford J, Wesevich J, Simons D (1997) A plasticity concrete material model for DYNA3D. Int J Impact Eng 19(9–10):847–873
Malvar LJ, Crawford JE, Morrill KB (2000) K&C concrete material model release III – automated generation of material model input, TR-99-24.3. Karagozian & Case, Structural Engineers, Glendale, CA
McGlaun JM, Thompson MG, Elrick MG (1990) CTH: a three-dimensional shockwave physics code. Int J Impact Eng 10:351–360
McMichael LM, Noble C, Margraf J, Glascoe L (2009) Fully-coupled blast effects modeling of large critical infrastructure. ASCE fifth congress on forensic engineering, LLNL-CONF-411649, November 10–15
Morris J (2004) Thunder science runs: simulation of hard and deeply buried targets using LDEC, UCRL-PRES-206648
Morris J, Johnson S (2009) Dynamic simulations of geological materials using combined FEM/DEM/SPH analysis. Geomech Geoeng 4(1):91–101
Neuscamman S, Glenn L, Schebler G, McMichael L, Glascoe L (2011a) Simulating small-scale experiments of in-tunnel airblast using STUN and ALE3D. LLNL-TR-498891
Neuscamman S, Glenn L, Glascoe L (2011b) A fast-running, physics-based tool for explosives in tunnels: model validation. Paper presented at 82nd Shock & Vibration Symposium, October 31–November 3, Baltimore, Maryland. LLNL-PRES-509019
Nichols AL, The ALE3D team (2009) Users manual for ALE3D, An arbitrary Lagrange/Eulerian 2D and 3D code system, Volume 2, Material and chemical models, Lawrence Livermore National Laboratory, UCRL-SM-404490
Noble C, Kokko E, Darnell I, Dunn T, Haggler L, Leininger L (2005) Concrete model descriptions and summary of benchmark studies for blast effects simulations. Lawrence Livermore National Laboratory, UCRL-TR-215024
Noble CR, Wemhoff AP, McMichael LD (2008) Thermal-structural analysis of the MacArthur Maze Freeway collapse. ASME 2008 summer heat transfer conference, Jacksonville, FL, August 10–14, 2008
Perret WR (1968) Free field ground Motion in granite. Report No.POR-4001. Sandia Laboratory, Albuquerque, New Mexico
Rubin MB, Vorobiev OY, Glenn LA (2000) Mechanical and numerical modeling of a porous elastic-viscoplastic material with tensile failure. Int J Solids Struct 37:1841–1871
Schock RN, Heard HC, Stephens DR (1973) Stress–strain behavior of a granodiorite and two graywackes on compression to 20 Kilobars. J Geophys Res 78(26):5922–5941
Souers P, Anderson S, Mercer J, McGuire E, Vitello P (2000) JWL++: a simple reactive flow code package for detonation. Propell Explos Pyrotech 25:54–58
Thrun R, Goertner JF, Harris GS (1993) Underwater bubble collapse against a flat plate. 1992 Seneca Lake test series data report, 1993, NSWCDD/TR-92/482
Vorobiev O, Antoun T (2011) Equivalent continuum modeling for nonlinear wave propagation in jointed media. Int J Numer Meth Eng 86:1101–1124. doi:10.1002/nme.3094
Vorobiev O, Lomov I, Antoun T (2005) Numerical simulation of wave propagation in jointed rock media. In: Oñate E, Owen DRJ (eds) Eighth international conference on computational plasticity, Barcelona, 2005

http://www.springer.com/978-1-4614-7266-7

Blast Mitigation
Experimental and Numerical Studies
Shukla, A.; Rajapakse, Y.D.S.; Hynes, M.E. (Eds.)
2014, VIII, 364 p., Hardcover
ISBN: 978-1-4614-7266-7